https://doi.org/10.1038/s44304-025-00129-9

Estimation of cascading hydroclimatic hazard impacts on supply systems and associated economic shocks

Marlon Vieira Passos [1,2] ✉, Jung-Ching Kan [1,2,4], Georgia Destouni [2,3,4], Karina Barquet [1,4], Luigia Brandimarte [2,4] & Zahra Kalantari [2,3,4]

Emerging systemic risks driven by climate extremes and societal vulnerabilities are causing considerable damage to supply systems and overall economies. In this study, we combined hydroclimatic hazard impact and supply-driven input-output models to develop an integrated approach for estimating the cascading impacts on food, electricity, and water supply associated with droughts, floods, and heatwaves. National-level results for Sweden indicate moderate to strong associations between annual supply variables and monthly climate indices ($0.39 \leq R^2 \leq 0.62$) at municipal units. Economic modeling revealed losses in key sectors, such as agriculture, energy, and insurance. The results from this economic modeling show that combined hydroclimatic hazards between 2005 and 2022 inflicted €8.4 billion of economic damage on agriculture, electricity, and insurance. Of this, flood-related damage represented the largest share, totaling €4.1 billion, followed by drought-induced supply shortages (€2.9 billion), and heatwave impacts (€2.3 billion).

Infrastructure systems and their provision of critical services are vulnerable to direct and indirect impacts from hydroclimatic hazards, such as floods, droughts, and heatwaves[1,2]. The impacts of droughts and heatwaves on crop production in Europe have roughly tripled in the last five decades[3]. Droughts may also severely affect water supply for human consumption, causing detrimental effects to human health, raising safety concerns, and hindering societal development and sustenance[4]. Flooding due to heavy rain can cause widespread critical and social infrastructure damage, with projected increased hazards in many regions, including Asia and Africa. These hazards are due to changes in the climate, natural landscape, and society, such as economic and population growth[5]. When these impacts escalate across supply networks, it can lead to substantial economic losses. Consequently, improving our understanding and management of the systemic risks associated with cascading impacts that disturb the distribution of essential goods and services is are global priorities for sustainable development[6].

Impact modeling has been applied to estimate specific adverse effects from hydroclimatic hazards on supply systems. For instance, Zampieri et al. found that a composite drought and heatwave indicator explains more than 40% of inter-annual global crop yield[7]. A global study on drought impacts on hydropower production revealed that 67 out of 134 countries experience a reduction of over 20% in mean annual production once per decade[8]. Impacts of droughts on public water supply can be observed in some countries, including Germany and the UK, especially when severe and short drought events are combined with long but less intense dry periods[9]. Additionally, the impacts of floods on global crop production led to average decreases of 4% for soy, 3% for rice, 2% for wheat, and 1% for maize worldwide from 1982 to 2016[10].

The consequences of hydroclimatic hazards are typically investigated by modeling the relationships between supply anomalies and climate indices, assuming that variations from trends can be partially attributed to extreme environmental conditions[7–9]. Anomalies can be identified through a variety of detrending methods. These include linear regression, polynomial regression, locally weighted scatterplot smoothing, and moving average techniques[11]. The Palmer Drought Severity Index, Standardized Precipitation Index, Standardized Precipitation Evapotranspiration Index, and Standardized Streamflow Index[12] are examples of indices that can be utilized to evaluate occurrence, intensity, and duration of various drought types. Similarly, climate indices have been developed for heatwave and flood hazards. Considering the 90th percentiles of maximum temperature on each calendar day as thresholds, a Heatwave Intensity Index was implemented to assess potential impacts on human health and economic activities[13]. The Daily Flood Index (DFI) was created to monitor flood hazards based on daily effective precipitation[14].

[1]Stockholm Environment Institute, Stockholm, Sweden. [2]Department of Sustainable Development, Environmental Science and Engineering, KTH Royal Institute of Technology, Stockholm, Sweden. [3]Department of Physical Geography, Stockholm University, Stockholm, Sweden. [4]These authors contributed equally: Jung-Ching Kan, Georgia Destouni, Karina Barquet, Luigia Brandimarte, Zahra Kalantari. ✉e-mail: marlonvp@kth.se

Several economic models have been applied to quantify monetary impacts from natural hazards, emphasizing the need to implement mitigation measures of extreme events on society[15]. A common approach for economic disaster impact analysis is the use of input-output (I-O) models. These consider fixed monetary transactions between sectors to capture cascading supply shocks and computable general equilibrium models, which incorporate supply and demand elasticities through more sophisticated assumptions[16]. Integrated assessment models use projections from global climate models to estimate the impacts of climate change on specific systems, employing methods such as cost-supply curves[17], damage functions[18], or optimization models[19], depending on the sector and model design. Numerous empirical approaches have been developed to assess economic impacts from natural hazards[20]. For instance, a hydro-economic optimization model was employed to assess the impacts of climate-induced droughts on water resources and hydroelectricity generation in the Upper Euphrates Basin, using historical hydrological data and drought indices[21].

Current impact models primarily focus on linear relationships between anomalies and hazards[22]. But many impacts are nonlinear, with thresholds where damage escalates disproportionately, potentially underestimating impacts and misleading stakeholders[23]. Minor anomalies may have negligible consequences, but extreme anomalies can lead to systemic breakdowns. Moreover, current approaches primarily focus on isolated impacts within specific sectors, such as agriculture, water supply, or energy production. However, there is limited understanding as to how disruptions from extreme events in one sector propagate through supply systems and spread to other sectors[24].

This study aims to combine hydroclimatic hazard impact models with supply-driven I-O models to present a holistic approach to assessing systemic impacts induced by drought, floods, and heatwave hazards. To account for impact nonlinearity, polynomial fitting was employed, and systemic impact propagation was modeled using economic I-O analysis driven by spatially aggregated impacts. The following research questions (RQs) were explored in applying this approach:

- How are hydroclimatic indices and anomalies of supply variables associated?
- What are the average patterns between indices and anomalies?,
- How are anomalies distributed at different hazard classification thresholds?
- What are the cascading economic losses due to hydroclimatic hazard impacts?

In this study, the approach presented was applied at national and municipal levels for the example case of Sweden. Although Sweden is relatively well-insulated from hydroclimatic hazards due to its geographic and climatic conditions, considerable economic impacts have occurred, for example, from the Gudrun cyclone in 2005[25] and the heatwaves and droughts of 2018[26]. From 2005 to 2020, 80% of the total freshwater water withdrawal in the country was, on average, obtained from surface water[27]. Between 2001 and 2020, hydropower accounted for an average of 44% of total national electricity production[28]. Additionally, over 90% of the agricultural crop production in the country was rainfed[29]. Regarding climate change, there is a wetting-warming trend with increasing flood and compound drought-heatwave hazards in many areas[30]. These characteristics indicate vulnerabilities in the Swedish economy to hydroclimatic hazards. In particular, given the generally low risk memory for such events[31], societal preparedness to manage both their direct impacts and their cascading effects remains limited, in comparison to countries with a longer history and greater experience of extreme events[32]. Global studies also indicate that approximately 75-81% of human freshwater use is withdrawn from surface water[33], and hydropower is the main source of energy in more than 35 countries[34]. This demonstrates that vulnerabilities similar to those in Sweden are present in many regions, making the Swedish case study a relevant example worldwide. The data-driven framework presented in this manuscript can identify systemic economic impacts that are often overlooked or underreported in vulnerable nations, thereby supporting policymaking and investment in climate resilience.

The Results section first addresses the hazard impact and supply-driven economic shock analyses in relation to the research questions posed. In the Discussion section, we evaluate the findings compared to existing literature, provide implications for hydroclimatic hazard management, discuss limitations, and offer suggestions for future developments.

Results

Hydroclimatic hazard impact modeling

The relationships between the statistically significant modeled and detected annual anomalies of total crop yield, streamflow, and hydropower production in Swedish municipalities (290 in total) are shown in Fig. 1. Drought, flood, and heatwave hazards are represented by the Standardized Precipitation and Evapotranspiration Index with a 12-month accumulation period (SPEI12), Daily Flood Index (DFI), and Heatwave Intensity Index (HWI), respectively. The highest nonlinear associations were found between the SPEI12 and streamflow (R^2 = 0.62), indicating the relatively high influence of precipitation rates on surface water discharge. The weakest overall associations were observed between the HWI and streamflow and hydropower production (R^2 = 0.39). The overall coefficient of determination values suggests that the climate indices, when aggregated into calendar monthly maximums, have a moderate ability to explain the variance of observed supply anomalies relevant to water, food, and electricity supply. The values of root mean squared error (RMSE) remain lower than the standard deviations, indicating that the anomaly models perform relatively well in estimating annual hydroclimatic hazard anomalies.

Figure 2 presents ensemble averages of modeled nonlinear relationships between hazard indices and anomalies of supply variables at Swedish municipality levels. Prediction intervals indicate much larger variability in anomaly estimates under more extreme conditions. Drier periods represented as negative SPEI12 values are mostly associated with negative supply anomalies, indicating adverse impacts. With severely dry conditions (SPEI = −1.5), the modeled average anomalies on crop production, streamflow, and hydropower production are −16%, −41%, and −26%, respectively. The associations of heatwave intensities with crop yield demonstrate an overall negative net effect under both extremely hot and extremely cold conditions. The associations of high HWI with both streamflow and hydropower production are net positive, although substantial variability exists among municipalities. There is an overall indication that increased flood hazards are associated with reduced crop productivity.

For each hazard-supply variable pairwise combination, the distributions of annual observed impacts were aggregated for low, moderate, and extreme hazard classification thresholds at statistically significant regions, as shown in Fig. 3. In general, negative crop production anomalies were found under drier conditions. Streamflow and hydropower energy supply generally decrease during moderate and extreme drought conditions, while the opposite patterns occur during elevated flood hazards. The largest negative impacts were seen in the case of droughts on streamflow and hydropower production, with median anomalies of −27% and −23%, respectively. Extreme heatwave conditions are associated with negative crop yield anomalies.

Cascading economic shocks from hydroclimatic impacts

Using the average impacts attributed to the entire country as the initial shocks in a national-level Input-Output (I-O) model, the propagated economic supply shocks and associated total losses to Gross Value Added (GVA) were estimated over the entire study period, with the latest I-O table from 2022 considered as the baseline. Table 1 lists the economic sectors most affected by hydroclimatic hazards with at least 10 million euros in annual losses from 2005 to 2022. The losses and relationships between sectors are shown in Fig. 4.

The total annual economic losses to the GVA are summarized in Sweden from 2005 to 2022 due to supply shocks in water, food, and electricity systems, as well as property damage from flood hazards. Combined

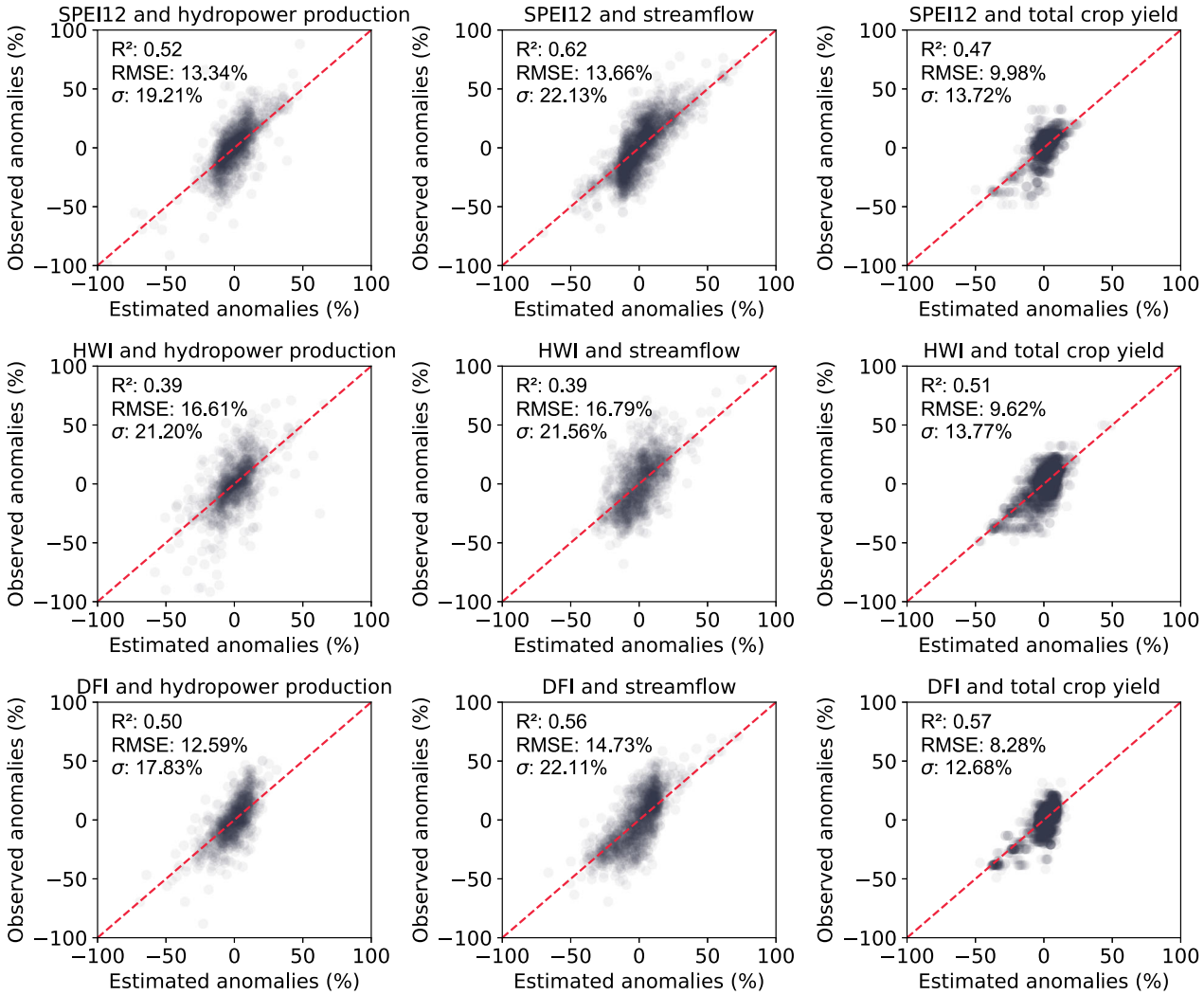

Fig. 1 | Relationships between estimated and observed anomalies of supply variables using climate indices for each hazard-anomaly pairwise combination. SPEI12, HWI, and DFI represent drought, heatwave, and flood hazards, respectively. Each data point represents one annual anomaly in a municipality.

losses correspond to the total sum of losses associated with hazards in individual municipalities. Considerable flood-related economic impacts were observed in several years, notably in 2005 and 2021. Droughts also contributed heavily to losses, particularly in 2013, 2016 to 2018, and 2022. Flood impacts, mostly those causing property damage, represented the largest losses due to hydroclimatic hazards over the study period, accounting for 4.1 billion euros in total. Supply shortages caused by droughts constituted 2.9 billion euros in losses and heatwave impacts amounted to approximately 2.3 billion euros.

The economic sectors with major annual losses above 10 million euros due to supply shocks are shown, with arrows indicating the size of indirect, propagated losses to the GVA in one sector caused by a shock in another sector. These figures refer to 2005, 2013, 2018, and 2021. These were the four years with the largest combined losses during the period considered. The losses in 2005 were predominantly due to extensive damage caused by Cyclone Gudrun[25], with the insurance sector experiencing the highest direct losses, with cascading effects on other industries, such as real estate and electricity. 2013 had a unique combination of drought and flood impacts in different regions. The supply shock was mainly driven by reductions in hydropower production and water supply due to droughts, estimated using impact modeling. Floods and droughts led to losses of approximately 200 million euros in the insurance sector and 137 million euros in the electricity sector, respectively. In 2018, the supply shocks were initiated by the agricultural sector. This was due to an aggregated 10% total crop yield loss nationwide resulting from a historically hot and dry season. The agricultural losses considerably escalated towards other sectors, especially food production activities. In 2021, a 5.5% decrease in crop yield associated with combined hydroclimatic hazards and infrastructure losses of 440 million from floods comprise substantial economic losses in that year. In general, the energy and insurance sectors were the most directly affected by hydroclimatic hazards. Regarding indirect effects, the results revealed that secondary losses were particularly severe in the real estate sector, which experienced greater overall losses than the primarily affected sectors of agriculture and water supply. This is due to strong real estate dependencies on electricity, food, and water provision for its normal operations.

Discussion

Regarding the association between hydroclimatic indices and anomalies in supply variables (RQ1), the modeling approach shows moderate associations and demonstrates that potential impacts can be estimated at varying degrees of confidence. Connections have previously been studied between drought and heatwave indices and crop yield[7], drought and streamflow[35], and drought and hydropower production[36]. This study expands on the impact investigation for other hazard-supply combinations involving heatwave and flood hazards, as well as including property damage. The analysis shows that the impact of climate indices on supply varies by location, resolved at finer scale than the national. In most Swedish municipalities, annual anomalies can be linked to extreme events by comparing

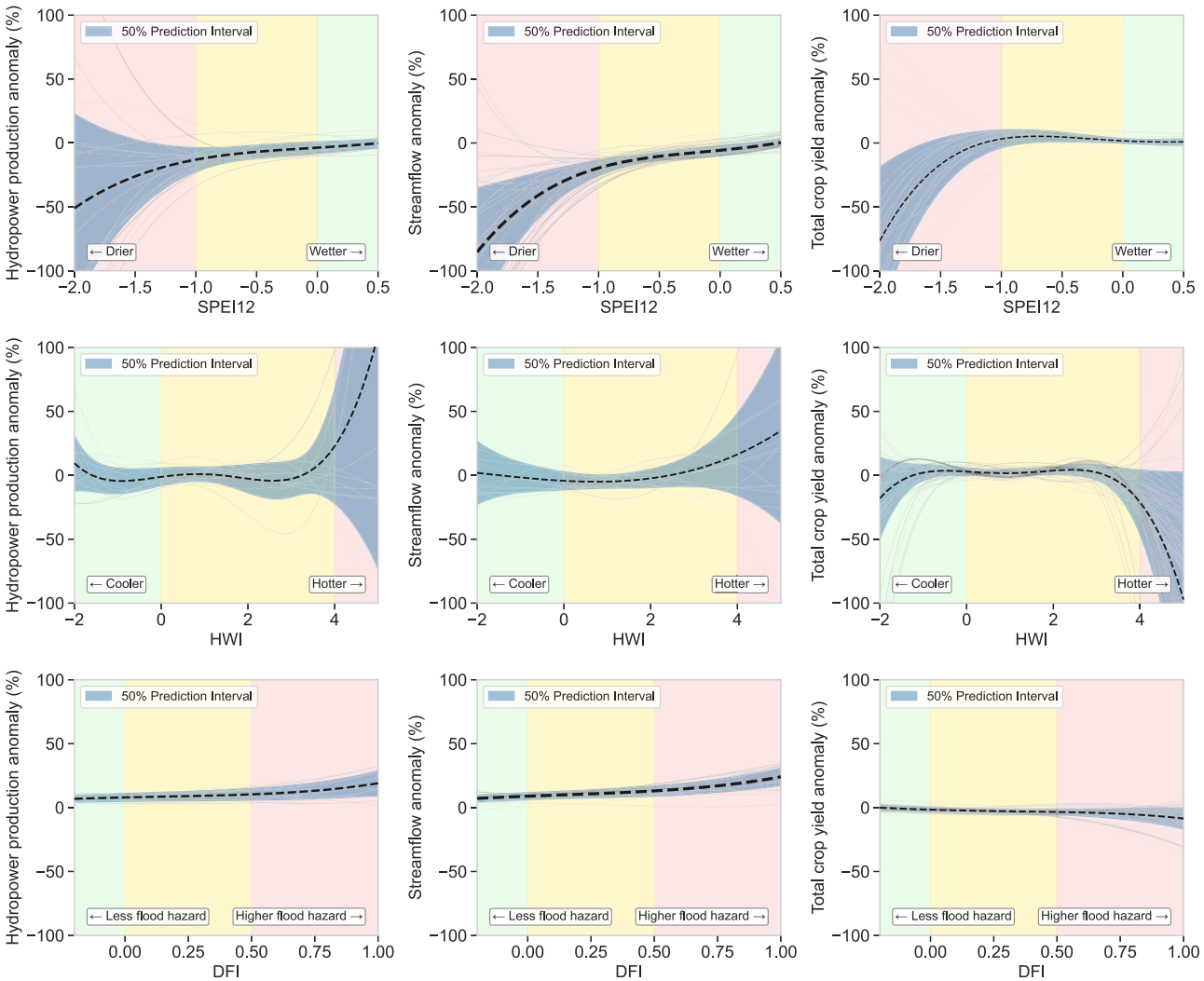

Fig. 2 | Ensemble average plots of modeled relationships between hydroclimatic hazard indices and supply variables, only for climate index values under hazard conditions. SPEI12, HWI, and DFI measure drought, heatwave, and flood hazards, respectively. Colored bands indicate threshold levels: green for low, yellow for moderate, and red for extreme. Solid lines represent fitted models for each municipality, with thickness and transparency weighted by local cross-validated R^2. Dashed lines represent the average model estimations for all Swedish municipalities.

nonlinear patterns with the highest monthly index values for each month of the year. The hazard impact models generated, when applied in real time, can be used for impact forecasting using climate indices[37]. This development is crucial for making early warning systems more impact-based rather than merely providing information about hazard conditions. This, consequently, makes risk management more effective[38]. It is important to note that while the regression analysis conducted in this study shows the strength of associations between hazards and potential impacts, this is not sufficient to establish causality. Establishing causal relationships would require the application of inference methods using control variables, such as multivariate regression analysis[39] or propensity score matching[40].

When examining the average patterns between indices and anomalies (RQ2), drought effects exhibit the most consistently negative associations with supply variables. This is due to their well-known impacts on productive sectors[41]. Observed anomalies associated with heatwaves have a net average negative effect on food supply, even though their impact on total crop yield can be both positive and negative depending on the region. These findings are consistent with previous research showing that heat stress can cause positive or negative impacts for different crop types[42] in relatively cold and wet regions[43–45]. In Sweden, with approximately 19% of the average annual streamflow regulated[46], overall patterns show that water and hydropower electricity supply are still vulnerable to harmful hydroclimatic conditions. This implies that policymakers should consider impact mitigation strategies, especially in the south of the country, which has been a historical drought hotspot[30]. Preventive measures to mitigate drought impacts on the water-food-energy nexus involve solutions such as green infrastructure for water harvesting[47], strengthening cross-regional energy integration[48], and robust planning of the role of hydropower in the energy transition[49]. Additionally, a water balance analysis that accounts for all significant inputs and outputs of water to and from the surface water and groundwater systems and any interactions between them is necessary. This is particularly acute for a country like Sweden, where there is a knowledge gap of how major changes in the energy industry will potentially change hydropower reservoir operation practices[49].

When analyzing how supply anomalies are distributed across different types of hydroclimatic hazards (RQ3), the framework demonstrates that the supply anomaly classification using climate indices can be useful for understanding the supply impacts and risks associated with various hydroclimatic hazards. A similar technique has been applied for drought impacts in crop yields under a range of conditions[50]. The findings show that supply shortages can vary considerably between moderate and extreme conditions for the same hazard due to the nonlinearity of supply anomaly-

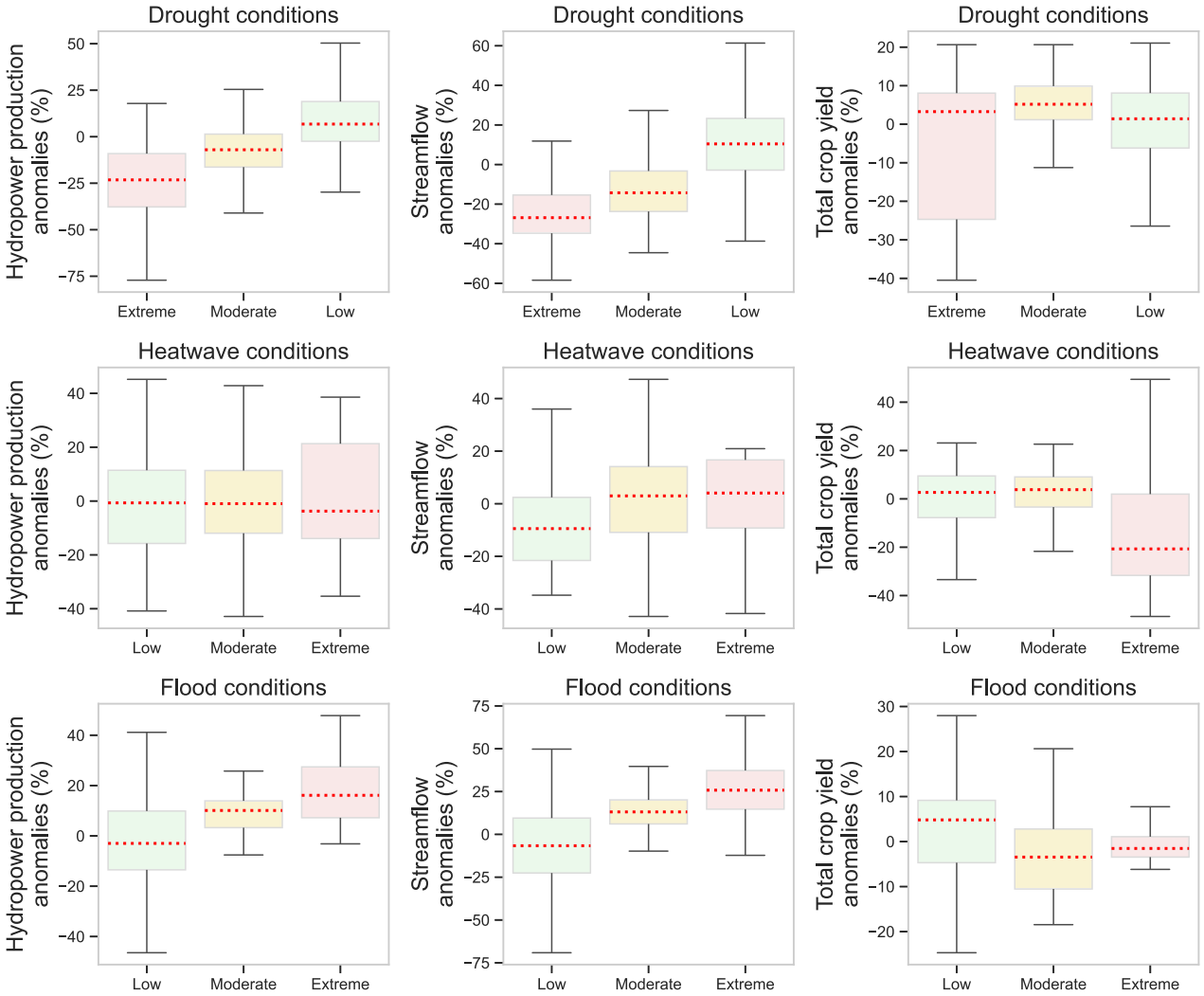

Fig. 3 | Distribution of annual anomalies detected in municipalities under different hydroclimatic conditions. Median values are represented as dotted red lines.

Table 1 | Critical sectors affected by hydroclimatic hazards based on the I-O analysis

Code	Industry
ACCO	Accommodation and food service activities
AETA	Architectural and engineering activities
AGRI	Crop and animal production, hunting, and related service activities
CARE	Residential care activities and social work activities without accommodation
CONS	Construction
EDUC	Education
ENGY	Electricity, gas, steam, and air conditioning supply
FOOD	Manufacture of food products; beverages and tobacco products
HLTH	Human health activities
IRPF	Insurance, reinsurance, and pension funding, except compulsory social security
LAMC	Legal and accounting activities; activities of head offices; management consultancy
PADM	Public administration and defense; compulsory social security
REAL	Real estate activities
WHOL	Wholesale trade; except of motor vehicles and motorcycles
WSUP	Water collection, treatment, and supply

hazard relationships[23,51]. For instance, as shown in Fig. 3, moderate drought and heatwave conditions appear to improve crop yield productivity in most areas, in consistency with previous observation-based findings[52]. If these conditions persist over time and are extreme, however, yields generally decline[44]. The number of samples of potential hazardous events increased considerably by incorporating not only extreme hazard categories but also moderate ones, allowing for more nuanced distinction of impacts at different categories. Negative impacts on hydropower production and streamflow due to moderate droughts show that even regions with highly regulated flows are vulnerable to adverse effects even during relatively mild droughts[53].

When estimating cascading economic losses caused by hydroclimatic hazard impacts (RQ4), our framework combining the I-O and impact models proved useful to obtain reasonable figures regarding direct and indirect impacts. This framework can help planners compare the costs of implementing mitigation measures, such as integrated water resource management and resilient cropping systems[54], against the benefits of reducing potential future losses. I-O modeling was applied in this study to quantify direct economic losses from the impacts of hydroclimatic hazards on supply sectors. This model also quantified indirect losses using sectoral relationships based on national accounts data. Although relatively few sectors trigger supply shocks, indirect effects were quantified for many sectors, providing useful insights into systemic risks for planners. The resultant monetary values can also serve as reference points to support affected groups, such as farmers. The validity of this approach was evaluated

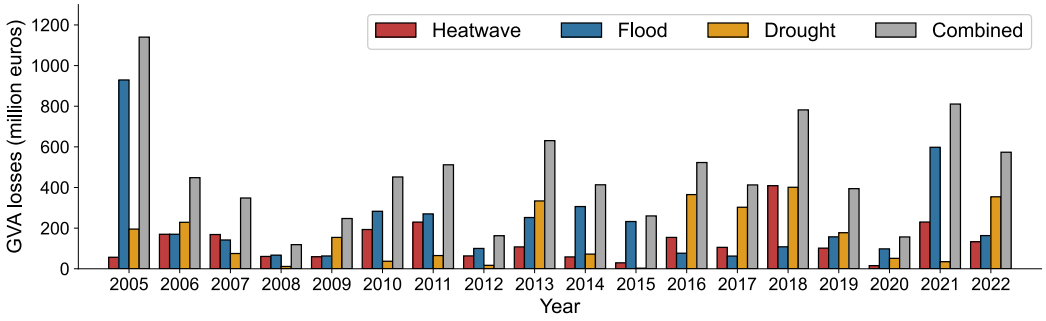

(a) Annual losses to GVA (Gross Value Added) in Sweden (2005-2022) associated with hydroclimatic hazards and flood property damage.

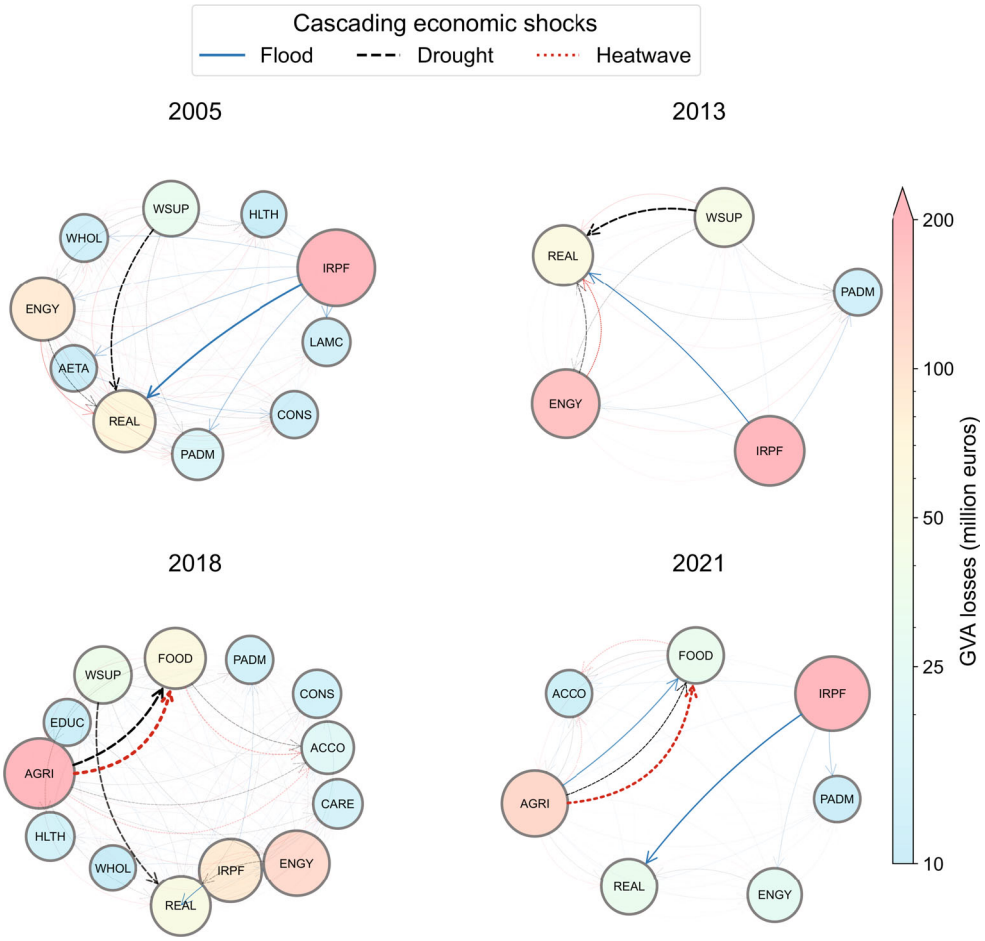

(b) Propagation of yearly sectoral economic shocks (2005, 2013, 2018, 2021) from drought, flood, and heatwave events (see legend). Arrow thickness and transparency indicate shock magnitude between sectors; node color shows direct GVA loss. Acronyms: ACCO (Accommodation), AETA (Architecture/Engineering), AGRI (Agriculture), CARE (Social Care), CONS (Construction), EDUC (Education), ENGY (Utilities), FOOD (Food/Beverage), HLTH (Healthcare), IRPF (Insurance/Pension), LAMC (Legal/Accounting), PADM (Public Administration), REAL (Real Estate), WSUP (Water Supply), WHOL (Wholesale). See Table 1 for full titles.

Fig. 4 | Results from the I-O analysis at national level. Impacts of hydroclimatic hazards on GVA (**a**) and propagation of economicshocks through sector networks (**b**).

by comparing the estimated economic impacts against similar assessments at national and European levels. The economic loss of 674 million euros due to compound droughts and heatwaves in 2018, equivalent to 6914 million SEK using the yearly average conversion factor of 10.26[55], falls within the estimate of 6000 to 10,000 million SEK according to the Swedish Board of Agriculture[56]. Monetary losses attributed to the multi-year drought from 2016 to 2019 are of a similar order of magnitude to estimations reported by several European countries, including the Czech Republic, Germany, and Poland[26]. Results indicate that economic impacts from energy and water supply shortages were considerable, as seen in 2013 and 2022. However,

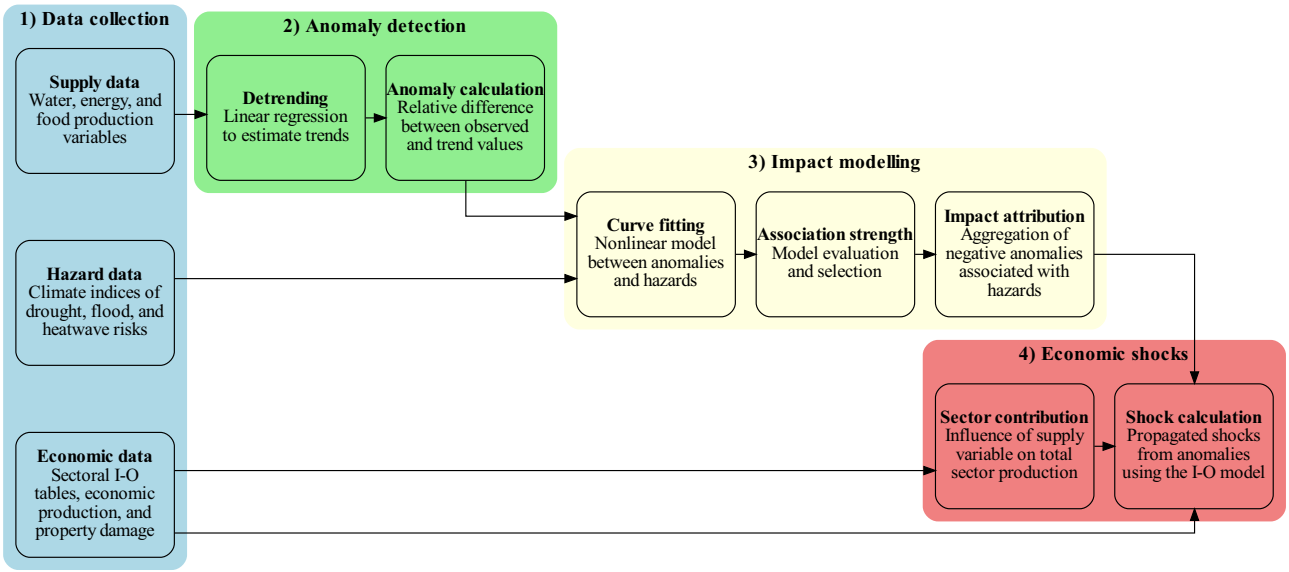

Fig. 5 | Methodological flowchart representing the study framework.

these impacts are rarely quantified or included in damage reports to the same extent as agricultural losses. This suggests a gap in how disaster impacts are measured, potentially leading to an incomplete understanding of total economic losses. Given hydropower's dominance in Sweden's electricity sector, direct and indirect drought losses represented 39% of total impacts, a figure comparable to the 48% observed in the European boreal region between 1990 and 2016[57]. Moreover, losses in Sweden's water supply sector accounted for 12% of total drought impacts, in contrast to the 14% estimated at the European level[57]. Since losses associated with flood hazards on water, electricity, and food provision were relatively minor, the economic I-O model integrated insurance damage losses on property, allowing for a more holistic comparison between hazards. Results in Fig. 4e show that flood impacts on properties were the main driver of economic losses from hydroclimatic hazards in Sweden, reaching 0.24% of GDP in 2005. This is close to the mean disaster cost of the Emergency Events Database (EM-DAT) sample[58].

The availability and quality of input data, particularly for socio-economic impacts, are limiting factors for the accuracy of this study. Datasets representing supply systems and infrastructure impacts have much lower temporal and spatial resolution than those for hydroclimatic hazards. Moreover, economic and supply data may be unavailable for modeling in data-scarce regions[59]. Relying solely on historical hazard-anomaly relationships at annual scales may also overlook socio-demographic shifts and long-term factors, such as behavioral changes or migration patterns[60] that could either amplify or diminish the overall supply effects. The approach presented in this paper considers publicly available flood damage impacts through insurance claims from property owners. This dataset does not include impacts on infrastructure beyond buildings, such as roads and dams, which underestimates the total economic losses. Moreover, the supply-driven I-O model applied in this study relies on simplifying assumptions of economic dynamics[61]. For instance, it does not consider the import or export of goods between countries, which would represent transboundary effects of the hazard impacts[62]. Another limitation of the economic model relates to the level of aggregation within the national I-O table. The agricultural sector, for example, encompasses both crop production and livestock raising. The analysis quantifies the economic shock on other sectors from hazard-induced losses in major crops, but these crops are partially used as feed for the livestock industry. Since both sub-sectors are combined, the I-O model does not capture the intra-sectoral shock propagation where a reduction in crop supply directly impacts livestock production through feed availability and cost.

The results call for future studies to further apply and test the approach developed here for other parts of the world, considering also alternative datasets of supply and damage impacts, other than from official sources, by using techniques such as automation, machine learning, and natural language processing. The supply impacts detected through this approach can also be applied to infrastructure system modeling to evaluate cascading effects on water and electricity distribution systems, along with disruptions to food supply chains. Apart from losses to sectoral gross value added, the supply-driven I-O model could be further expanded to analyze price changes due to supply constraints caused by hydroclimatic hazards.

Methods

The methodological framework for estimating hydroclimatic hazard impacts consists of four main steps: (1) Data collection; (2) Anomaly detection; (3) Impact modeling; and (4) Economic shocks. Climate indices representing hazard conditions, supply variables, and economic input-output data were analyzed to estimate impacts from shortages on a national scale. To illustrate how this framework can be applied, Sweden was selected as the study region. The framework flowchart is shown in Fig. 5. Each major framework step is described in this section.

Data collection

This study uses datasets of supply, hazard, and economic variables from multiple sources in order to identify potential socio-economic impacts associated with hydroclimatic hazards. The most suitable climate indices to represent drought, flood, and heatwave conditions in the study region were selected by comparing their long-term hazard detection performance against secondary historical reports[30]Table 2 summarizes all datasets utilized in this study.

To represent surface water supply, mean annual streamflow rates from the Vattenwebb database[63] were obtained by averaging all stations located within the municipal boundaries. As a proxy for food provision, annual agricultural productivity was assessed using a multi-step approach. First, for each of the most common crop types in Sweden[64] (including wheat, potatoes, oat, corn, barley, and productive grasslands such as ley for total harvest), its actual yield in a given region and year was calculated as harvested mass per unit area. This actual yield was then compared to an average baseline yield established for that specific crop type across the dataset, resulting in a standardized performance index for each crop. Finally, these individual crop performance indices were aggregated into an overall regional productivity index, where each crop's contribution was weighted by its harvested area in that region and year. Energy supply was represented as

annual hydropower production per municipality[28]. Linear interpolation was implemented to fill temporal data gaps in crop yield and hydropower production.

Heatwave hazards were accounted for using the Heatwave Intensity Index (HWI) developed by the European Drought Observatory considering anomalies of daily maximum air temperatures[13]. Drought hazards were indicated by the Standardized Precipitation and Evapotranspiration Index (SPEI) with a 12-month accumulation period[65], while flood hazards were conveyed by the Daily Flood Index (DFI)[14], based on daily precipitation rates. These climate indices were derived using regional datasets and demonstrated good accuracy for detecting extreme hydroclimatic events in Sweden from 1922 to 2021[30]. Hazard index values were spatially averaged in each municipality using zonal statistics[66] to match the resolution of the supply variables. Table 3 shows the thresholds indicating hydroclimatic hazard conditions for each climate index. The thresholds distinguishing low from moderate conditions (set at 0 for all indices) were derived from the original literature: DFI[14], SPEI[65], and HWI[13]. The thresholds distinguishing moderate from extreme conditions are set as the 95 percentiles of the value distributions, as shown in Fig. 6.

Full International and Global Accounts for Research in Input-Output analysis (FIGARO)[67] was used for economic impact modeling at the national scale. The most recently available input-output table, corresponding to 2022, was chosen as the base period for the supply shock analysis. To estimate the economic contributions from selected supply variables within their corresponding sectors, total water withdrawal by type[27], economic results from the agricultural sector[68], and electricity use statistics[69] were applied.

Table 2 | Summary of the datasets employed in this study

Category	Variable	Unit	Reference
Economy	FIGARO EU input-output table	million euros	67
Economy	Total water withdrawal by type	thousand m^3	27
Economy	Agricultural economic results	million SEK	68
Economy	Electricity supply and use	GWh	69
Economy	Insured property damage claim	SEK	77
Economy	Currency exchange rates	SEK to euros	55
Hazard	Standardized Precip. Evapo. Index (SPEI12)	–	30
Hazard	Heatwave Intensity Index (HWI)	∘C	30
Hazard	Daily Flood Index (DFI)	–	30
Supply	Hydropower production	MWh	28
Supply	Average streamflow	m^3/s	63
Supply	Total harvest per crop	tons	64
Supply	Agricultural land area per crop	hectares	64

Table 3 | Hazard classification thresholds adopted for the Daily Flood Index (DFI), Heatwave Intensity Index (HWI), and Standardized Precipitation and Evapotranspiration Index (SPEI)

Climate Index	Threshold	Description
DFI	<0	Low flood hazard
	0 to 0.5	Moderate flood hazard
	≥0.5	Extreme flood hazard
HWI	<0	Low heat intensity
	0 to 4	Moderate heat intensity
	≥4	Extreme heat intensity
SPEI	≤−1.0	Extreme drought conditions
	−1.0 to 0	Moderate drought conditions
	>0	Low drought conditions

Anomaly detection and impact modeling

To identify variations in supply variables possibly associated with hydroclimatic factors, annual anomalies were calculated for each municipality over the study period. A detrending supply time series was performed to reduce effects from long-term demand changes or technological advances[70], reduce sources of non-climatic bias, and isolate sudden variations caused by short-term events, such as hydroclimatic hazards.

Simple linear regression was applied to fit temporal supply variable trends. Given the supply variable value y_i and the fitted trend $\hat{y}_i$ at time i, the relative anomalies θ_i were determined as

$$\theta_i = \frac{y_i - \hat{y}_i}{\hat{y}_i} \times 100\%. \quad (1)$$

To assess the relationships between supply shocks and hazards, models fitting detected anomalies and climate indices were generated at the municipality scales. The anomaly models were defined as polynomials ranging from first to fourth order in the form:

$$\hat{\theta}_i = f(I_i) = aI_i^4 + bI_i^3 + cI_i^2 + dI_i + e, \quad (2)$$

Where $\hat{\theta}_i$ is the estimated anomaly, and $f(I_i)$ is a function of the climate index I at time i. The fitting parameters a, b, c, d, and e were estimated using the least squares method by minimizing the expression

$$\sum_{i=1}^{n} \left(\theta_i - f(I_i)\right)^2. \quad (3)$$

Lower and upper parameter bounds of −10 and 10, respectively, were applied to constrain the anomaly predictions within a reasonable range. The trust region reflective method[71] was the adopted solving algorithm to optimize the estimation parameters, respecting the established bounds. The

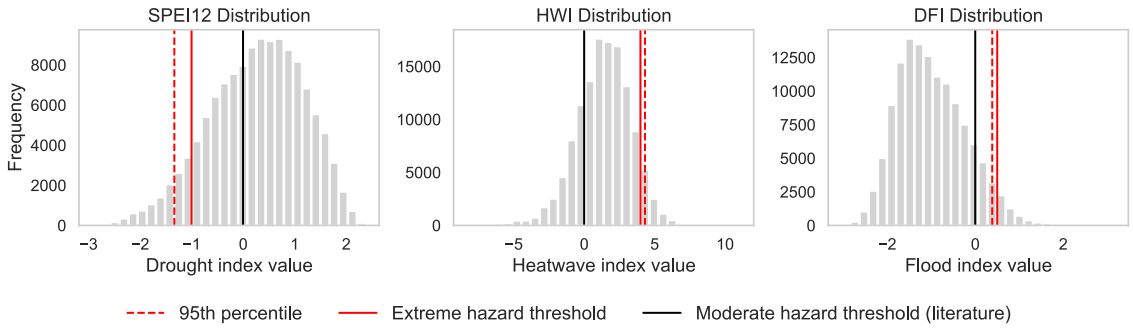

Fig. 6 | Distribution of annual climate indices along municipalities and corresponding classification thresholds for moderate and extreme hazard conditions.

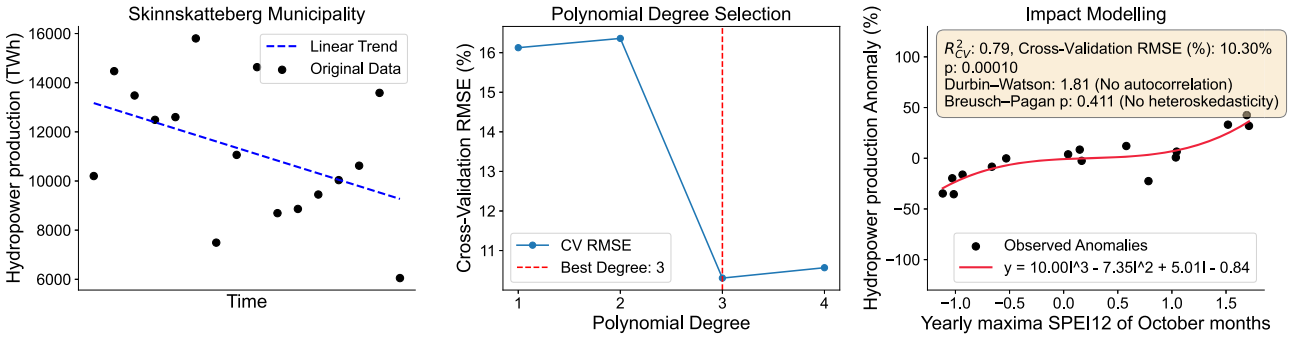

Fig. 7 | Example of anomaly detection in annual hydropower production in the Skinnskatteberg municipality (left), selection of optimal polynomial degree (middle), and modeling of anomalies using monthly maximum SPEI12 values for the month of October each year (right).

algorithm was implemented through the "curve_fit" function from the Python package "SciPy"[72].

To maximize the strength of hazard-impact relationships, the models were fitted for a combination of annual anomalies and maximum annual climate indices for each calendar month over the study period. This better reflects the seasonal and short and medium-term character of the hazards and their possible impacts, increasing the confidence of predictions for particular months of the year. The daily indices HWI and DFI were aggregated into monthly maximum values. To develop a robust regression model for each municipality while mitigating the risk of overfitting, a hyperparameter tuning procedure was implemented to select the optimal polynomial degree. For each municipality's dataset, polynomial models of degrees one through four were tested. The model selection was performed using a 5-fold cross-validation (CV) strategy. In this process, the data was randomly partitioned into five folds. For each candidate degree, a model was iteratively trained on four folds and validated on the remaining hold-out fold. This was repeated until every fold had served as the validation set. The out-of-sample predictions from all folds were then aggregated to compute a single cross-validated Root Mean Squared Error (CV-RMSE) for that degree. The polynomial degree that yielded the lowest CV-RMSE was selected as the optimal model complexity for that specific municipality. This data-driven approach ensures that the chosen model generalizes well to unseen data by penalizing overly complex models that would otherwise fit to noise in the training set. The cross-validated coefficient of determination (CV-R^2) was calculated for the aggregated set of observed values and their corresponding out-of-sample predictions. The most representative monthly models in each municipality for each hazard-anomaly combination were selected based on the highest CV-R^2 values[73]. This empirical approach allows the identification of seasonal effects such as the most influential period of water availability on the aggregated crop yield, accounting for spatial variations without relying on generalized growing season assumptions. Figure 7 demonstrates the application of the anomaly detection and modeling method for annual hydropower production in the Skinnskatteberg municipality from 2005 to 2022, which showed the highest CV-R^2 among all municipalities for this variable pair. In this example, a third-order polynomial was chosen to minimize out-of-sample prediction errors. The results indicate the potential influence of harsher drought conditions on electricity output from the municipality.

The F-test was performed to test the significance of the fitted model at 5% significance level. The Durbin-Watson test was applied to assess autocorrelation in the residuals, considering values between 1.5 and 2.5 as indicative of no significant autocorrelation. To evaluate the assumption of homoskedasticity, the Breusch-Pagan test was employed at 5% significance level. Negative anomalies detected with statistically significant associations with supply variables exceeding moderate hazard thresholds (Table 3) were considered as effective hydroclimatic hazard impacts. The negative impacts were subsequently annually aggregated at the national level to serve as inputs for the economic model. This aggregation was conducted through weighted averaging across all municipalities, using absolute supply values as weights to ensure that municipal production contributions were appropriately accounted for in the national average.

Economic shocks

Supply side I-O modeling[74,75] was performed to quantify how initial shocks due to droughts, floods, and heatwaves propagate through the national economy, indirectly affecting various economic sectors. The model was implemented using the 2024 edition of the FIGARO I-O tables, comprising 64 industries[67]. The dataset comprises 27 EU countries and 18 non-EU countries. However, only data pertaining to Sweden was used in this study. Consequently, the influence of imports and exports has not been considered. The economic model describes the total output X produced for each economic sector c as

$$X_c = Z_{1c} + Z_{2c} + \ldots + Z_{nc} + v_c, \tag{4}$$

where Z_{rc} is the intermediate input from sector r to sector c, provided in the dataset, and v is the sectoral gross valued added (GVA). Introducing unit vector $\mathbf{i}$, expression (4) can be represented in vector form as:

$$\mathbf{X}' = \mathbf{i}'\mathbf{Z} + \mathbf{v}'. \tag{5}$$

By dividing intermediate production by total production, allocation coefficients b_{rc} are defined as

$$b_{rc} = \frac{Z_{rc}}{X_r}. \tag{6}$$

An allocation coefficient b_{rc} represents the total output generated in sector c for each unit of primary input from sector r[74]. Replacing equation (6) in the previous equation (5) yields

$$\mathbf{X}' = \mathbf{X}'\mathbf{b} + \mathbf{v}'. \tag{7}$$

This can be rewritten as

$$\mathbf{X}' = \mathbf{v}'(\mathbf{I} - \mathbf{b})^{-1} = \mathbf{v}'\mathbf{O}, \tag{8}$$

where $\mathbf{I}$ and $(\mathbf{I}-\mathbf{b})^{-1}$ are the identity matrix and the inverse matrix of output allocation $\mathbf{O}$[76], respectively. The expression

$$\Delta\mathbf{X}' = \Delta\mathbf{v}'\mathbf{O} \tag{9}$$

is used to capture how the initial supply shock $\Delta\mathbf{v}'$ caused by a hydroclimatic hazard leads to a decrease in total output from different sectors.

Considering the latest input-output table for 2022 as the base year, annual shock scenarios were simulated using the spatially aggregated negative impacts on food, water, and energy supply due to hydroclimatic

Table 4 | Estimated supply variable contributions on economic sectors

Economic sector (shortened title)	Crop yield	Discharge rates	Hydropower production	Reference
Agriculture (AGRI)	44%	–	–	68
Utilities (ENGY)	–	–	44%	28
Water supply (WSUP)	–	80%	–	27

hazards. Each supply anomaly initially affects a corresponding economic sector, multiplied by its allocated contributions from national statistics. The contributions of total crop yield to the agricultural sector were calculated as the average fraction of these over the total sectoral value from 2008 to 2019[68]. The average hydropower share of total electricity production in Sweden from 2001 to 2022 was adopted as the contribution in this sector[28]. The contribution from streamflow rates on the water supply sector was estimated as the proportion of surface water withdrawal compared to the total freshwater supply[27]. The resultant fixed sectoral contributions for the supply variable are listed in Table 4. To estimate flood-related property damage, insurance claims were incorporated explicitly, attributed to storm and water-related natural hazards into the economic model[77]. The underlying data are compiled and published by Insurance Sweden, based on annual reporting by member insurance companies. These statistics include only claims that insurers have classified under the classification types storm or water, as defined in the national insurance reporting framework. The storm category includes damages resulting from high wind events and snowstorms, while the water category includes damages caused by torrential rain, prolonged precipitation, snowmelt, and rising water levels in lakes or rivers. The insurance claims considered in the dataset cover several categories of insurance products, including home insurance, vacation home insurance, boat insurance, business and property insurance, and other general insurance types. These insurance products provide coverage for damage to physical property, loss of income, and liability across households, businesses, and boats. Only claims that insurers explicitly attributed to the defined storm or water-related hazards are included. Claims resulting from unrelated causes, such as pipe bursts due to freezing temperatures or house fires, are not captured in the dataset unless the insurer classified the cause as a storm or water-related event. This approach ensures that the insurance data used in the model represents a focused estimate of insured economic losses specifically attributable to flood hazards. Since property damage is not a supply variable with estimated anomalies, the monetary losses were directly included in the model, as a cascading loss initiating in the insurance sector (IRPF). For comparative purposes, four distinct shock types were analyzed each year, one for each hazard and a combined case.

Data availability

The hazard-related datasets applied in this manuscript can be accessed at https://doi.org/10.6084/m9.figshare.28100255.

Code availability

The code used to reproduce this study is available online and can be accessed via the link https://doi.org/10.5281/zenodo.16793775.

Received: 14 April 2025; Accepted: 15 July 2025;
Published online: 15 August 2025

References

1. Wang, S., Ancell, B., Yang, Z.-L., Duan, Q. & Anagnostou, E. N. Hydroclimatic extremes and impacts in a changing environment: Observations, mechanisms, and projections. *J. Hydrol.* **608**, 127615 (2022).
2. Kumar, N., Poonia, V., Gupta, B. & Goyal, M. K. A novel framework for risk assessment and resilience of critical infrastructure towards climate change. *Technol. Forecast. Soc. Change* **165**, 120532 (2021).
3. Brás, T. A., Seixas, J., Carvalhais, N. & Jägermeyr, J. Severity of drought and heatwave crop losses tripled over the last five decades in Europe. *Environ. Res. Lett.* **16**, 065012 (2021).
4. Orimoloye, I. R., Belle, J. A., Olusola, A. O., Busayo, E. T. & Ololade, O. O. Spatial assessment of drought disasters, vulnerability, severity and water shortages: A potential drought disaster mitigation strategy. *Nat. Hazards* **105**, 2735–2754 (2021).
5. Merz, B. et al. Causes, impacts and patterns of disastrous river floods. *Nat. Rev. Earth Environ.* **2**, 592–609 (2021).
6. UNDRR. A framework for global science in support of risk-informed sustainable development and planetary health. https://www.undrr.org/publication/framework-global-science-support-risk-informed-sustainable-development-and-planetary (2021).
7. Zampieri, M., Ceglar, A., Dentener, F. & Toreti, A. Wheat yield loss attributable to heat waves, drought and water excess at the global, national and subnational scales. *Environ. Res. Lett.* **12**, 064008 (2017).
8. Wan, W., Zhao, J., Popat, E., Herbert, C. & Döll, P. Analyzing the impact of streamflow drought on hydroelectricity production: a global-scale study. *Water Resour. Res.* **57**, e2020WR028087 (2021).
9. Stagge, J. H., Kohn, I., Tallaksen, L. M. & Stahl, K. Modeling drought impact occurrence based on meteorological drought indices in Europe. *J. Hydrol.* **530**, 37–50 (2015).
10. Kim, W., Iizumi, T., Hosokawa, N., Tanoue, M. & Hirabayashi, Y. Flood impacts on global crop production: Advances and limitations. *Environ. Res. Lett.* **18**, 054007 (2023).
11. Meng, H. & Qian, L. Performances of different yield-detrending methods in assessing the impacts of agricultural drought and flooding: A case study in the middle-and-lower reach of the Yangtze River, China. *Agric. Water Manag.* **296**, 108812 (2024).
12. Vicente-Serrano, S. M. et al. Performance of Drought Indices for ecological, agricultural, and hydrological applications. *Earth Interact.* **16**, 1–27 (2012).
13. Lavaysse, C. et al. Towards a monitoring system of temperature extremes in Europe. *Nat. Hazards Earth Syst. Sci.* **18**, 91–104 (2018).
14. Deo, R. C., Byun, H.-R., Adamowski, J. F. & Kim, D.-W. A real-time flood Monitoring Index based on daily effective precipitation and its application to Brisbane and Lockyer Valley Flood Events. *Water Resour. Manag.* **29**, 4075–4093 (2015).
15. Botzen, W. J. W., Deschenes, O. & Sanders, M. The economic impacts of natural disasters: a review of models and empirical studies. *Rev. Environ. Econ. Policy* **13**, 167–188 (2019).
16. Galbusera, L. & Giannopoulos, G. On input-output economic models in disaster impact assessment. *Int. J. Disaster Risk Reduct.* **30**, 186–198 (2018).
17. Gernaat, D. E. H. J. et al. Climate change impacts on renewable energy supply. *Nat. Clim. Change* **11**, 119–125 (2021).
18. Burke, M., Hsiang, S. M. & Miguel, E. Global non-linear effect of temperature on economic production. *Nature* **527**, 235–239 (2015).
19. Emmerling, J. et al. The WITCH 2016 model - documentation and implementation of the shared socioeconomic pathways. Nota Di Lavoro 42.2016, Fondazione Eni Enrico Mattei (FEEM), Milano. https://hdl.handle.net/10419/142316 (2016).
20. Lazzaroni, S. & Van Bergeijk, P. A. Natural disasters' impact, factors of resilience and development: A meta-analysis of the macroeconomic literature. *Ecol. Econ.* **107**, 333–346 (2014).
21. Tuna, M. C., Aytac, A. & Dogan, M. S. Using an integrated hydro-economic model to determine the drought and energy relationship in

the Upper Euphrates Basin. *J. Water Clim. Change* **15**, 3346–3360 (2024).
22. Schewe, J. et al. State-of-the-art global models underestimate impacts from climate extremes. *Nat. Commun.* **10**, 1005 (2019).
23. Ruane, A. C., Phillips, M., Jägermeyr, J. & Müller, C. Non-linear climate change impacts on crop yields may mislead stakeholders. *Earth's. Future* **12**, e2023EF003842 (2024).
24. OECD. *Managing Climate Risks, Facing up to Losses and Damages: Understanding, Reducing and Managing Risks*. https://www.oecd.org/en/publications/managing-climate-risks-facing-up-to-losses-and-damages_55ea1cc9-en.html. (OECD, 2021)
25. Mäll, M., Suursaar, Ü., Nakamura, R. & Shibayama, T. Modelling a storm surge under future climate scenarios: Case study of extratropical cyclone Gudrun (2005). *Nat. Hazards* **89**, 1119–1144 (2017).
26. Moravec, V. et al. Europe under multi-year droughts: How severe was the 2014–2018 drought period? *Environ. Res. Lett.* **16**, 034062 (2021).
27. Statistiska centralbyrån. Total water withdrawal by type of water and region. Every fifth year 1970–2020. http://www.statistikdatabasen.scb.se/ (2024).
28. Statistiska centralbyrån. Elproduktion och bränsleanvändning (MWh) efter region, produktionssätt, bränsletyp och år. http://www.statistikdatabasen.scb.se/ (2024).
29. Grusson, Y., Wesström, I. & Joel, A. Impact of climate change on Swedish agriculture: Growing season rain deficit and irrigation need. *Agric. Water Manag.* **251**, 106858 (2021).
30. Vieira Passos, M., Kan, J.-C., Destouni, G., Barquet, K. & Kalantari, Z. Identifying regional hotspots of heatwaves, droughts, floods, and their co-occurrences. *Stoch. Environ. Res. Risk Assess.* **38**, 3875–3893 (2024).
31. Barquet, K. et al. Variations of riskification: Climate change adaptation in four European cities. *Risk Hazards Crisis Public Policy* **15**, 491–517 (2024).
32. Englund, M. & Barquet, K. Threatification, riskification, or normal politics? A review of Swedish climate adaptation policy 2005–2022. *Clim. Risk Manag.* **40**, 100492 (2023).
33. Hanasaki, N., Yoshikawa, S., Pokhrel, Y. & Kanae, S. A global hydrological simulation to specify the sources of water used by humans. *Hydrol. Earth Syst. Sci.* **22**, 789–817 (2018).
34. Kaygusuz, K. Hydropower as clean and renewable energy source for electricity generation. *J. Eng. Res. Appl. Sci.* **5**, 359–369 (2016).
35. Bachmair, S., Kohn, I. & Stahl, K. Exploring the link between drought indicators and impacts. *Nat. Hazards Earth Syst. Sci.* **15**, 1381–1397 (2015).
36. Naumann, G., Spinoni, J., Vogt, J. V. & Barbosa, P. Assessment of drought damages and their uncertainties in Europe. *Environ. Res. Lett.* **10**, 124013 (2015).
37. Wang, Q. et al. A comprehensively quantitative method of evaluating the impact of drought on crop yield using daily multi-scale SPEI and crop growth process model. *Int. J. Biometeorol.* **61**, 685–699 (2017).
38. AghaKouchak, A. et al. Toward impact-based monitoring of drought and its cascading hazards. *Nat. Rev. Earth Environ.* **4**, 582–595 (2023).
39. Alexopoulos, E. C. Introduction to multivariate regression analysis. *Hippokratia* **14**, 23–28 (2010).
40. Benedetto, U., Head, S. J., Angelini, G. D. & Blackstone, E. H. Statistical primer: Propensity score matching and its alternatives†. *Eur. J. Cardio-Thorac. Surg.* **53**, 1112–1117 (2018).
41. Fleming-Muñoz, D. A., Whitten, S. & Bonnett, G. D. The economics of drought: A review of impacts and costs. *Aust. J. Agric. Resour. Econ.* **67**, 501–523 (2023).
42. Deryng, D., Conway, D., Ramankutty, N., Price, J. & Warren, R. Global crop yield response to extreme heat stress under multiple climate change futures. *Environ. Res. Lett.* **9**, 034011 (2014).
43. Li, W. et al. Contrasting drought propagation into the terrestrial water cycle between dry and wet regions. *Earth's. Future* **11**, e2022EF003441 (2023).
44. Orth, R., Destouni, G., Jung, M. & Reichstein, M. Large-scale biospheric drought response intensifies linearly with drought duration in arid regions. *Biogeosciences* **17**, 2647–2656 (2020).
45. Fabri, C., Moretti, M. & Van Passel, S. On the (ir)relevance of heatwaves in climate change impacts on European agriculture. *Clim. Change* **174**, 16 (2022).
46. Arheimer, B. & Lindström, G. Electricity vs Ecosystems – understanding and predicting hydropower impact on Swedish river flow. *Proc. Int. Assoc. Hydrol. Sci.* **364**, 313–319 (2014).
47. Kalantari, Z., Ferreira, C. S. S., Keesstra, S. & Destouni, G. Nature-based solutions for flood-drought risk mitigation in vulnerable urbanizing parts of East-Africa. *Curr. Opin. Environ. Sci. Health* **5**, 73–78 (2018).
48. Zhao, X., Huang, G., Li, Y. & Lu, C. Responses of hydroelectricity generation to streamflow drought under climate change. *Renew. Sustain. Energy Rev.* **174**, 113141 (2023).
49. Xylia, M., Bin Ashraf, F. & Barquet, K. Hydropower development in the energy transition: Perspectives from northern Sweden. Tech. Rep., Stockholm Environment Institute. https://www.sei.org/publications/hydropower-energy-transition-northern-sweden/ (2023).
50. Li, Y., Guan, K., Schnitkey, G. D., DeLucia, E. & Peng, B. Excessive rainfall leads to maize yield loss of a comparable magnitude to extreme drought in the United States. *Glob. Change Biol.* **25**, 2325–2337 (2019).
51. Ding, Y. et al. Nonlinear effects of agricultural drought on vegetation productivity in the Yellow River Basin, China. *Sci. Total Environ.* **948**, 174903 (2024).
52. Orth, R. & Destouni, G. Drought reduces blue-water fluxes more strongly than green-water fluxes in Europe. *Nat. Commun.* **9**, 3602 (2018).
53. Brunner, M. I. Reservoir regulation affects droughts and floods at local and regional scales. *Environ. Res. Lett.* **16**, 124016 (2021).
54. Rahman, G., Jung, M.-K., Kim, T.-W. & Kwon, H.-H. Drought Impact, Vulnerability, Risk Assessment, Management and Mitigation under Climate Change: A Comprehensive Review. *KSCE J. Civil Eng.* 100120. https://www.sciencedirect.com/science/article/pii/S122679882405267X (2024).
55. ECB. Euro exchange rates charts. https://www.ecb.europa.eu/stats/policy_and_exchange_rates/euro_reference_exchange_rates/html/eurofxref-graph-sek.en.html (2024).
56. Jordbruksverket. Långsiktiga effekter av torkan 2018. https://webbutiken.jordbruksverket.se/sv/artiklar/ra1913.html (2019).
57. Naumann, G., Cammalleri, C., Mentaschi, L. & Feyen, L. Increased economic drought impacts in Europe with anthropogenic warming. *Nat. Clim. Change* **11**, 485–491 (2021).
58. EIOPA. *Climate Change, Catastrophes and the Macroeconomic Benefits of Insurance*. https://data.europa.eu/doi/10.2854/407671. (Publications Office, LU, 2021).
59. Malgwi, M. B., Fuchs, S. & Keiler, M. A generic physical vulnerability model for floods: review and concept for data-scarce regions. *Nat. Haz. and Earth Sys. Sci*. **20**, 2067–2090 (2020).
60. Naqvi, A. & Monasterolo, I. Assessing the cascading impacts of natural disasters in a multi-layer behavioral network framework. *Sci. Rep.* **11**, 20146 (2021).
61. Oosterhaven, J. *Supply-Driven IO Quantity Model and Its Dual, Price Model*, 87–104 https://doi.org/10.1007/978-3-031-05087-9_7. (Springer International Publishing, Cham, 2022).
62. Hedlund, J. et al. Impacts of climate change on global food trade networks. *Environ. Res. Lett.* **17**, 124040 (2022).
63. SMHI. Vattenwebb. https://www.smhi.se/data/hydrologi/vattenwebb (2024).
64. Jordbruksverket. Hektar- och totalskörd efter Län, Gröda, Variabel, Tabelluppgift och År. https://jordbruksverket.se/statistik (2024).
65. Vicente-Serrano, S. M., Beguería, S. & López-Moreno, J. I. A Multiscalar Drought Index sensitive to global warming: the

standardized precipitation Evapotranspiration Index. *J. Clim.* **23**, 1696–1718 (2010).
66. Haag, S., Tarboton, D., Smith, M. & Shokoufandeh, A. Fast summarizing algorithm for polygonal statistics over a regular grid. *Comput. Geosci.* **142**, 104524 (2020).
67. Eurostat. FIGARO tables (2024 edition): Annual EU inter-country supply, use and input-output tables. https://ec.europa.eu/eurostat/web/esa-supply-use-input-tables/database (2024).
68. Jordbruksverket. EAA – Ekonomisk kalkyl för jordbrukssektorn, preliminär utveckling för 2022–2023. https://jordbruksverket.se/om-jordbruksverket/jordbruksverkets-officiella-statistik/jordbruksverkets-statistikrapporter/statistik/2024-02-13-eaa---ekonomisk-kalkyl-for-jordbrukssektorn.-preliminar-utveckling-for-2022-2023 (2024).
69. Statistiska centralbyrån. Electricity supply and use 2001–2022 (GWh). https://www.scb.se/en/finding-statistics/statistics-by-subject-area/energy/ (2024).
70. Hendrawan, V. S. A., Komori, D. & Kim, W. Possible factors determining global-scale patterns of crop yield sensitivity to drought. *PLOS ONE* **18**, e0281287 (2023).
71. Branch, M. A., Coleman, T. F. & Li, Y. A subspace, interior, and conjugate gradient method for large-scale bound-constrained minimization problems. *SIAM J. Sci. Comput.* **21**, 1–23 (1999).
72. Virtanen, P. et al. SciPy 1.0: Fundamental algorithms for scientific computing in Python. *Nat. Methods* **17**, 261–272 (2020).
73. Mohammed, S. et al. Assessing the impacts of agricultural drought (SPI/SPEI) on maize and wheat yields across Hungary. *Sci. Rep.* **12**, 8838 (2022).
74. Miller, R. E. & Blair, P. D.*Input-Output Analysis: Foundations and Extensions* 2 edn https://www.cambridge.org/core/product/identifier/9780511626982/type/book. (Cambridge University Press, 2009).
75. Jenkins, K., Dobson, B., Decker, C. & Hall, J. W. An integrated framework for risk-based analysis of economic impacts of drought and water scarcity in England and Wales. *Water Resour. Res.* **57**, e2020WR027715 (2021).
76. Wu, K.-Y., Wu, J.-H., Huang, Y.-H., Fu, S.-C. & Chen, C.-Y. Estimating direct and indirect rebound effects by supply-driven input-output model: A case study of Taiwan's industry. *Energy* **115**, 904–913 (2016).
77. Insurance Sweden. Inträffade skador per år. https://www.svenskforsakring.se/statistik/skadeforsakring/hem--villa-foretags--och-fastighetsforsakring/intraffade-skador-per-ar/ (2024).

Acknowledgements

We are grateful for the financial support provided by the Swedish Research Council (VR) (grant numbers 2021-06309 and 2022-04672) and the Swedish Civil Contingencies Agency (MSB) and FORMAS (HydroHazards project).

Author contributions

Z.K., K.B., G.D., and L.B. conceived this study. M.V.P. collected the data, used the software, and carried out the formal analysis. K.B., Z.K., and G.D. acquired the funding. M.V.P., Z.K., and J.C.K. developed the methodology. KB and Z.K. administered the project. K.B, Z.K., L.B., and GD. carried out the supervision. All authors participated in writing this paper.

Funding

Open access funding provided by Royal Institute of Technology.

Competing interests

The authors declare no competing interests.

Additional information

Correspondence and requests for materials should be addressed to Marlon Vieira Passos.